2012 IEEE International Conference on Robotics and Automation
RiverCentre, Saint Paul, Minnesota, USA
May 14-18, 2012

Robust, Inexpensive Resonant Frequency Based Contact Detection for Robotic Manipulators

Spencer B. Backus, *Student Member, IEEE* and Aaron M. Dollar, *Member, IEEE*

Abstract — **This paper presents a method for detecting contact on a compliant link utilizing a method to sense changes in the resonant frequency of the link due to external contact. The approach uses an inexpensive accelerometer mounted on or inside the compliant link and a phase locked loop circuit to oscillate the link at its resonant frequency. Using this approach, we are able to reliably sense contact anywhere on the link with a contact force threshold sensitivity of between 0.05 and 0.15 N depending on the contact location.**

I. Introduction

TOUCH sensing continues to represent one of the most significant challenges to robotic manipulation. Although humans rely heavily on tactile sensing when grasping objects, the majority of robotic manipulators lack significant tactile sensors [1, 2]. Research efforts to develop novel sensors have spanned the range of both intrinsic/proprioceptive sensors and extrinsic/exteroceptive sensors (e.g. [3-7]).

In this work, we present a new approach to contact sensing, particularly useful for compliant, underactuated end-effectors such as the SDM Hand [8]. In general, the approach utilizes measurements of the frequency response of the digit in real time, with contact detection based upon a change in the resonant frequency. Unlike many traditional methods of sensing, which rely on expensive and oftentimes fragile custom-made sensors placed at the fingertips (or any surface where sensing is desired) [9], our approach uses a single, inexpensive accelerometer and a phase locked loop integrated circuit to excite the system at its resonant frequency. By sensing changes in this resonant frequency, we are able to detect contact anywhere on the digit.

Other researchers have investigated vibration-based contact sensors and applied similar frequency characterization techniques to systems, but have not combined the two in a frequency-based vibrational contact sensor. For example, Motoo et al. implemented an impedance-based contact sensor that consists of a two piezoelectric elements separated by a polymer sheet [3]. One of the piezoelectric elements is driven at a constant frequency while the other is used as a transducer to monitor the system's response. The signal from the piezoelectric element is used to measure the impedance of the polymer and contact is detected when the measured mechanical impedance changes. Rudolf and Seemann used a similar actuation scheme and a phase locked loop to oscillate a beam at resonance, but did not include sensing [10].

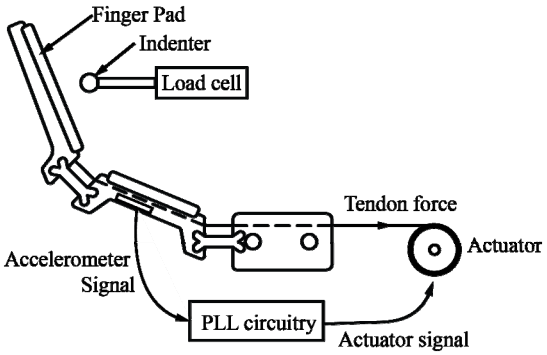

Fig. 1. Diagram of Instrumented finger system and test probe.

Imata and Terunuma have developed a closely related sensor for measuring the in vivo stiffness of human tissues[4]. This sensor consists of a piezoelectric driver and sensor mounted on a probe. The system is excited at its resonant frequency by a phase locked loop that tracks the resonant frequency of the probe. Stiffness of the contacted tissue is inferred based on the change in resonant frequency. This sensor has been developed into a commercial product, the Axiom Biosensor (Fukushima-ken, Japan).

In this paper, we utilize a similar resonant frequency tracking method in which we utilize an inexpensive accelerometer mounted within the proximal link of a compliant robotic finger (Fig. 1) and a phase locked loop circuit to drive the finger at its resonant frequency with its main flexion actuator. Using the accelerometer, we sense contact anywhere on the finger, detected when the frequency of resonant oscillation rises more than three standard deviations above the mean resonant frequency.

We begin this paper with a description of our approach, utilizing a simple beam and elastic contact model to illustrate the concept. Next, we describe our experimental setup and test procedure, followed by an evaluation of the proposed concept in a wide range of contact conditions and locations on the finger. Finally, we discuss issues related to the practical implementation of the approach, including how the results presented here can be extended to additional contact conditions as well as a richer information set about the contact state.

This work was supported in part by the National Science Foundation grant IIS-0953856.

S.B. Backus and A.M. Dollar are with the Department of Mechanical Engineering and Materials Science, School of Engineering and Applied Science, Yale University, New Haven, CT USA (e-mail: {spencer.backus, aaron.dollar}@ yale.edu).

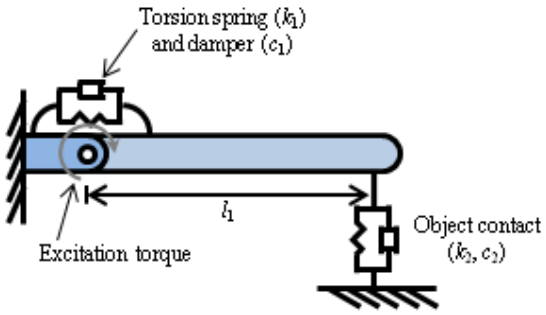

Fig. 2. Simple single link example model.

II. Approach

Our sensor operates by measuring the frequency response of the digit in real time and detects contact based upon observed changes in the resonant frequency. As shown in the single link and rotational joint example, Fig. 2, if a contact is modeled as a spring and damper in parallel acting at a point on the link, the stiffness and damping of the contact add to the stiffness and damping of the proximal joint and therefore change the overall stiffness of the system. As a result, the resonant frequency of the overall system changes as a function of both the location and stiffness of the contact. The sensor functions by detecting this change and thereby the underlying contact. Although the change in resonant frequency is a function of contact force and position, there is insufficient information to disambiguate which factor is responsible, making the sensor a purely binary measurement.

The following two equations represent the angular acceleration of the rotational joint and the resonant frequency of the link/contact system for small angles:

$$\ddot{\theta} = \frac{1}{I}\left(-(k_1 + k_2\ell_1^2)\theta - (c_1 + c_2\ell_1^2)\dot{\theta} + u(t)\right)$$

$$\omega_0 = \frac{1}{2\pi}\sqrt{\frac{k_1 + k_2\ell_1^2}{I}}\ Hz$$

where I is the link's moment of inertia, k_1 and c_1 are the spring and damping constants of the joint, k_2, c_2, and l_1 are the contact spring and damping constants and the contact location, and $u(t)$ is the excitation input. As expected, the resonant frequency is only a function of the two stiffnesses and the contact location, assuming the object is grounded or has a much higher inertia than the finger. When contact occurs, the contact stiffness term becomes non-zero and the resonant frequency shifts.

For the experimental system described later, $I = 1.2 \times 10^{-4}$ kg×m^2 and $k_1 = 2.5$ Nm/rad, resulting in an expected natural frequency (without contact) of approximately 23 Hz. For a stiff contact of $k_2 = 10{,}000$ N/m (the stiffness of the finger pad) and contact location $l_1 = 0.05$ m, the expected natural frequency shifts to approximately 76 Hz. For a very compliant contact of $k_2 = 100$ N/m and contact location $l_1 = 0.05$ m, the expected natural frequency shifts to approximately 24 Hz. However because of the positional constraint imposed on the digit by the tendon, the actual resonant frequencies with and without contact are somewhat different.

III. Experimental Methods

A. Experimental Setup

We have implemented this sensor on a two link polymer flexure-based finger derived from the SDM Hand design [8]. The digit, shown in Figs. 1 and 3, is actuated by a current-controlled DC motor (Maxon 2140.937-58.236-050) via a single distally-terminated tendon. This actuator applies both the force to flex the digit as well as the oscillatory force used to excite the digit at its resonant frequency. The digit is instrumented with a three axis accelerometer (model adxl335, Texas Instruments) embedded in the proximal link of the finger. Currently only the z axis is monitored and it is oriented normal to the finger pad.

Tracking of the resonant frequency in the physical system is achieved using a phase locked loop that measures the response of the finger and excites the digit at the resonant frequency. This is achieved by first measuring the oscillation of the proximal link of the digit normal to the finger pad with the accelerometer. Then, the accelerometer signal is filtered and digitized to meet the requirements of the phase locked loop integrated circuit (model cd4046be, Texas Instruments). First, the DC bias is removed from the signal by a second order high pass filter. This filter is implemented using a UA741 op-amp and has a cutoff frequency of 4.8 Hz. Then the signal is digitized using an op amp comparator implemented with a LM324 op-amp. The digital signal is then passed to the IC-based phase locked loop which generates the frequency of the excitation signal that drives the tendon actuator. The amplitude of the driving signal was adjusted so that the distal joint oscillates through approximately 0.9 degrees when not in contact with an object. This small amplitude oscillation is sufficient to generate a clear signal from the accelerometer but minimizes the displacement of the finger.

B. Contact Criteria

The criteria for contact detection is based upon a comparison of an initial base line sample collected during system initialization and the real time measurement of the oscillatory frequency of the digit, both of which are filtered using a 10 sample moving average. When powered on, the system is given 90 seconds to reach equilibrium, after which the mean and standard deviation of a one second sample of the frequency are measured. The frequency threshold indicative of contact is then set based on these two baseline measurements. Adjusting this threshold is a tradeoff between sensor sensitivity and accuracy: a lower threshold above the initial mean frequency results in greater sensitivity to extremely light contacts but also introduces a larger number of false positives. For th experiments presented in this paper, the frequency threshold is set as three standard deviations above the measured mean frequency. Contact is detected

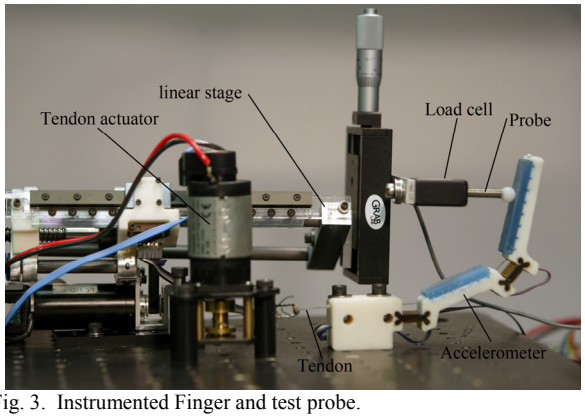

Fig. 3. Instrumented Finger and test probe.

when the real time measurement exceeds this preset threshold.

C. Test procedure

The sensor was evaluated based upon its ability to detect both initial contact events and its static contact state. In all trials, contact was made by a 0.25" diameter spherical nylon probe rigidly mounted to a linear stage. The loads exerted on the probe were also measured using a 5 lbf load cell (model MDB-5, Transducer Techniques).

To evaluate its ability to detect static contact events, the sensor was tested in three different static contact configurations: no contact where the probe did not contact the digit, light contact where the probe only contacted the finger for a portion of each oscillation, and full contact where the probe contacted the finger throughout each oscillation. These conditions were evaluated by applying each contact constraint and waiting for the system to reach equilibrium before recording a representative sample of its waveform and the observed resonant frequency.

The transient behavior of the system was measured by advancing a probe at a constant velocity until contact was detected. The sensor's performance is compared to direct contact detection based upon threshold contact force measurements taken at the same time using a load cell in series with the probe. Performance was quantified in terms of how far the probe advanced after contact was first measured by the load cell as well as measured contact force at the point when the sensor detected contact. This test was repeated for a range of velocities from 2.54 to 12.7 mm/sec (due to limitations with the current experimental setup) and over a range of contact locations both on the compliant finger pad and rigid back of the finger shown in Fig. 6.

IV. Results

The following two sections describe the results from the two experimental studies.

A. Static Behavior

In operation, the system exhibits one of three oscillatory behaviors depending on the contact condition, examples of which are shown in Fig 4. Without contact, the digit exhibits a clearly periodic oscillation with a dominant frequency of

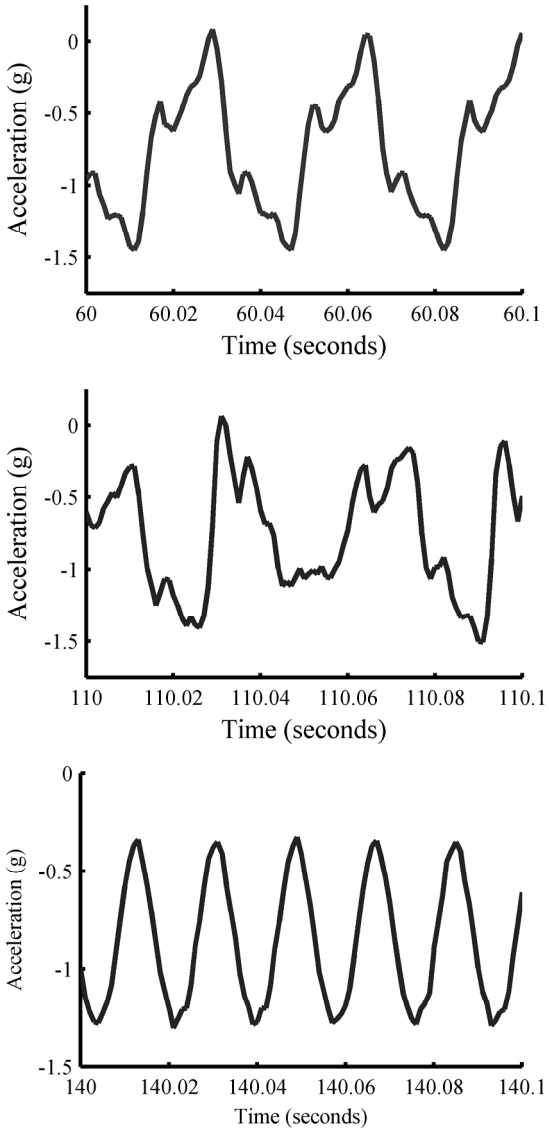

Fig. 4. Measured acceleration of the digit under no contact (top), light contact (middle), and full contact (bottom) conditions.

approximately 28 Hz. After contact is initiated but at low contact force on the order of 0.1 N, the system enters a bouncing contact regime where the digit only contacts the probe for a portion of its oscillation, due to limitations in the oscillation amplitude as well as the low stiffness of the finger. This regime is typified by more erratic oscillations and a small rise in resonant frequency to approximately 30 Hz. Lastly, with full contact, the link remains in contact throughout its full oscillation amplitude, during which the resonant frequency rises substantially to approximately 50 Hz.

B. Transient Behavior

In its current implementation, the described sensor is most useful in identifying the onset of contact on the finger. Fig. 5 shows a representative trial where the probe is advanced at 4.57 mm/sec and makes contact at the distal end of the

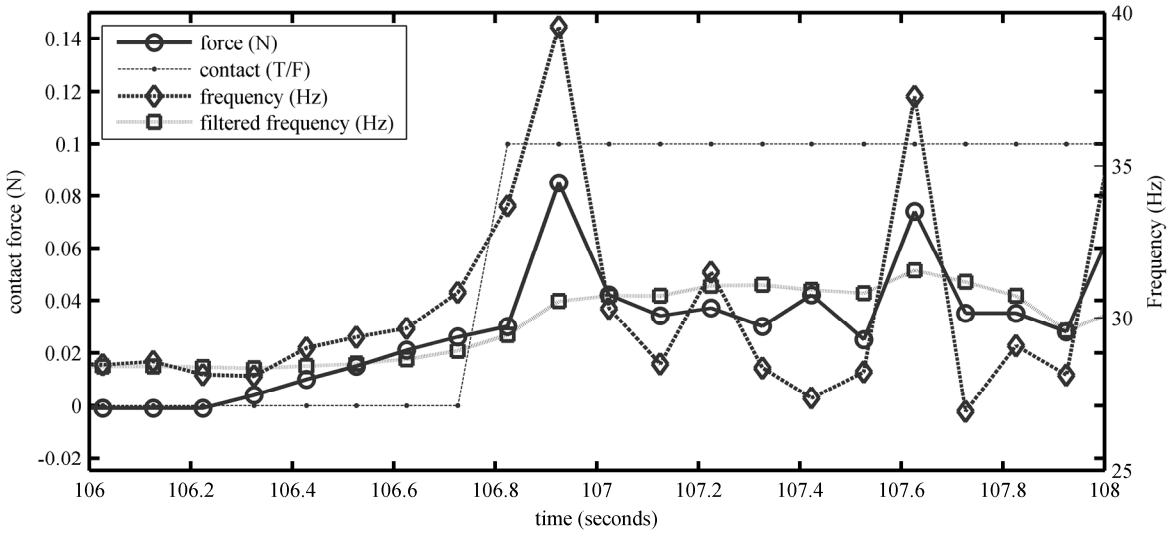

Fig. 5. Measured force, raw and filtered frequency, and contact state of the system for a representative contact trial. Contact is made at the distal end of the finger at 4.47 mm/sec.

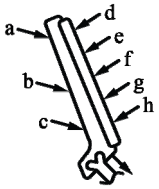

Fig. 6. Contact test locations.

TABLE I
SUMMARY OF TRANSIENT CONTACT TEST DATA

contact location		*micrometer position (mm)*	*speed (mm/sec)*	*Time (sec)*	*extent (mm)*	*force at contact (N)*
a	mean	19.05	3.785	0.33	1.372	0.111
	σ		0.159	0.15	0.599	0.017
b	mean	12.7	3.691	0.23	0.864	0.073
	σ		0.360	0.06	0.309	0.004
c	mean	0	4.919	0.20	1.067	0.057
	σ		0.103	0.00	0.051	0.006
d	mean	0	4.487	0.37	1.643	0.031
	σ		0.117	0.06	0.280	0.007
e	mean	6.35	4.885	0.43	2.252	0.050
	σ		0.082	0.06	0.338	0.006
f	mean	12.7	4.843	0.17	0.830	0.050
	σ		0.163	0.12	0.645	0.006
g	mean	19.05	4.555	0.37	1.710	0.075
	σ		0.374	0.15	0.776	0.014
h	mean	25.4	3.260	0.59	1.964	0.048
	σ		0.389	0.09	0.192	0.015
f	mean	12.7	2.540	0.20	0.576	0.038
	σ		0.305	0.00	0.059	0.005
f	mean	12.7	4.513	0.40	1.761	0.036
	σ		0.184	0.10	0.407	0.007
f	mean	12.7	6.435	0.23	1.524	0.032
	σ		0.249	0.06	0.440	0.007
f	mean	12.7	8.060	0.23	2.066	0.054
	σ		1.042	0.12	1.042	0.005
f	mean	12.7	10.685	0.17	1.880	0.072
	σ		0.089	0.06	0.616	0.027
f	mean	12.7	11.997	0.23	3.200	0.099
	σ		2.351	0.06	0.748	0.031

finger pad. In this trial, contact is registered by the load cell (i.e. force rises from 0 to 0.005 N) at t = 106.2 seconds. However contact detection based on the filtered frequency occurs 0.5 seconds later when the frequency rises above the threshold, at which point the contact force has risen to 0.03 N.

The aggregated results of a set of similar trials for various contact locations and velocities are presented in Table I and Figs. 7, 8, and 9. Figs. 7 and 8 show the effect of moving the contact location from the distal to the proximal end of the distal link of the finger on the back of the finger and finger pad, respectively, when the contact velocity is held constant at approximately 4.445 mm/sec. Similarly, Fig. 9 shows the effect of contact velocity on the sensor when contact is made in the middle of distal finger pad. As shown in these figures, the contact location and velocity both affect sensitivity. However, within the conditions we tested, the maximum expected force and displacement at contact detection is 0.15 N and 3.81 mm respectively. The contact force threshold is approximately 20 times better than the results achieved using the piezo film contact sensing scheme on a similar SDM finger presented in [5], although the contact velocity was not controlled in that study. This result also compares favorable with the performance of the commercially available Robotouch sensor, manufactured by Pressure Profile Systems and used in conjunction with the BarretHand and Willow Garage PR2 robots. This product has an advertized sensitivity of 0.1 psi on a 16 mm^2 element which corresponds to a sensitivity of approximately 0.01 N, but in practice this sensitivity is rarely able to be achieved due to mechanical noise associated with the motion of the robot and the common practice of covering the delicate sensors with compliant rubber finger pads that distribute contact forces over multiple elements.

V. DISCUSSION

A. Static Behavior

As can be seen in the three distinct responses under the three different static contact conditions, this sensor has the

potential to provide more than simple binary contact information. The increase in frequency and decrease in amplitude of the systems response between the light and full contact cases clearly correlates with the increase in contact force. However, our theoretical model predicts that both the location and object stiffness will also affect the resonant frequency of the full contact condition. Therefore while the additional information provided by the substantial frequency change that occurs between the light and full contact conditions may provide a useful indication of the relative contact force, it does not provide enough information to serve as a quantitative measure of contact force. However, this information combined with additional sensory knowledge (e.g. contact location on finger), might be able to provide useful information about contact force magnitude.

B. Dynamic Behavior

Although the system's ability to distinguish between static contact and non-contact states is useful, its ability to accurately detect the onset of contact is useful in many applications. As such we evaluated performance in terms of both the force threshold at which contact was sensed using the accelerometer and time delay between the onset (as sensed by the force transducer) and detection of contact.

One of the significant limitations of this sensor is its time response to contact events. As shown, the sensor takes on average 0.3 seconds to detect contact after it is registered by the load cell, during which time the probe has advanced and the contact force has increased noticeably. This time delay is a result of both the need to filter the frequency measurements as well as the magnitude of the frequency threshold. As can be seen in Fig. 5, the measured frequency rises substantially at the same time that the load cell first measures contact in the unfiltered signal. However, if contact detection is based on an unfiltered signal, the oscillations in the measured signal due to the erratic oscillations of the digit under light contact cause the sensor not to detect contact consistently. Similarly, if the frequency threshold is set low enough to detect this initial change in the filtered signal, the sensor suffers from a large number of false contact detections due to slow oscillations in the resonant frequency. Although not explored in this work, we plan to refine the system to reduce the noise in the frequency signal sufficiently to eliminate the need to filter it and thereby improve the time response of the sensor.

In addition to the time delay caused by the frequency threshold and filter, the Nyquist frequency dictates the maximum sampling rate of the system and limits the temporal resolution of the sensor to half of the lowest frequency of interest. Because the system oscillates at approximately 30 Hz, the sensor is limited to a maximum sampling rate of 15 Hz. However, the sampling frequency can be increased by exciting the digit at a higher harmonic frequency or to increase the stiffness of the digit, thereby increasing its resonant frequency. This in turn would allow us to better resolve the timing of contact detection by both the load cell and initial change in frequency.

In addition to the time delay between the onset and detection of contact, there appear to be two related trends in the data presented in Figs. 7, 8, and 9, both of which may stem from the time delay in contact detection discussed above. First, there is a positive correlation between the contact force and contact location. Secondly, there is a similar correlation between the contact velocity and the contact force threshold. Both trends can be explained by the constant time delay between onset of contact and contact detection caused by the filtering and thresholding of the frequency signal. This is most simply explained when contact velocity is varied: if the probe velocity is higher, the probe will have advanced further and deflected the finger

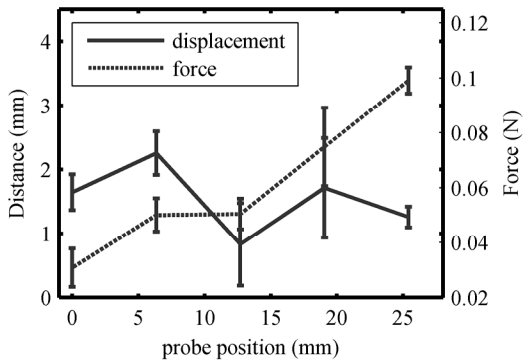

Fig. 7. Effect of contact location on the finger pad on measured contact force and displacement. Contact velocity is 4.445 mm/sec. while contact location is moved from the distal end of the finger (0) to towards the proximal end (1)

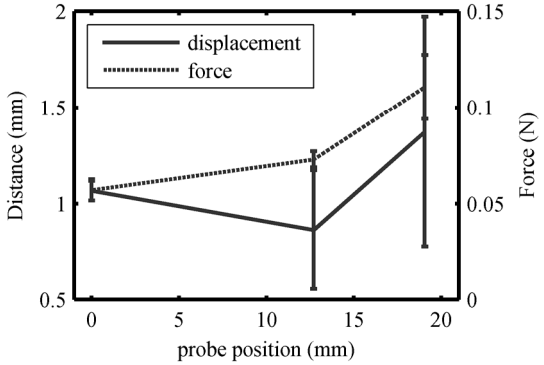

Fig. 8. Effect of contact location on the back of the finger on measured contact force and displacement. Contact velocity is 4.445 mm/sec. while contact location is moved from the distal end of the finger (0) to towards the proximal end (1)

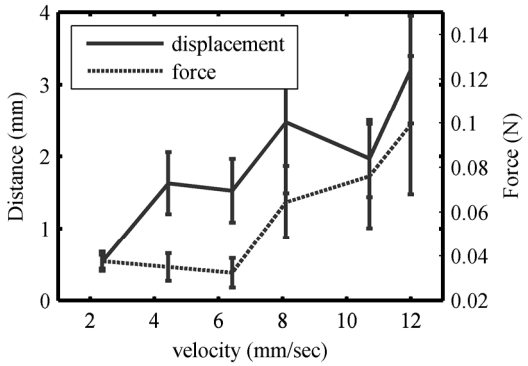

Fig. 9. Effect of contact velocity on measured contact force and displacement. Contact is made in the center of the distal finger pad while velocity is varied from 2.5 to 12.7 mm/sec.

more in the same amount of time. The greater finger deflection in turn results in a higher contact force. The observed trend for contact location can similarly be explained by the fact that for the given time delay the probe will advance the same distance regardless of contact location. However, moving the contact force's location proximally (towards the joint) reduces the moment arm at which it acts on the digit, increasing the force required to exert the same torque and acceleration on the finger.

C. Limitations and Future Work

The approach to contact sensing that we present here is a low cost contact sensing solution capable of detecting contact on both faces of a finger with a low force threshold and reasonable time response. However, it does suffer from a number of limitations in addition to those already discussed that, if addressed, would significantly expand its applicability.

One of the most significant limitations is that flexing the digit causes the resonant frequency of the digit to rise in a manner similar to a contact event. This means that if the sensor was used on a hand, as currently implemented (with a fixed threshold) it would not be useful once the fingers are flexed. This would make it useless for detecting contact when closing the fingers to grasp an object. However, it is possible to characterize the free resonant frequency of the finger as a function of tendon position and generate a frequency threshold for all possible tendon positions. This simple modification would then allow the contact sensor to function as the fingers are closed about an object.

Another limitation is that the excitation input is provided by the primary actuator. The current system uses a single backdrivable motor to both flex the finger and excite it. Although this can be beneficial in that an additional actuator is not needed for the system, it does impose a number of requirements on the motor, namely that it must be able to oscillate at the torque and frequency needed to excite the system. This requirement precludes the use of small low torque motors with large gear reductions. However because the sensor operates independent of excitation method it is possible to use two actuators, one such as a gear motor optimized for flexion of the digit and the other such as a fast acting solenoid for excitation in applications where a single larger gear motor is impractical.

In addition to these improvements and modifications, additional characterization of the system is needed to fully explore its applicability. One area that has not been explored yet is characterizing the sensor's response to contacts on the proximal link. Here we need to determine if the system responds in a similar manner to contacts on the proximal link and if the responses are distinct enough to differentiate between proximal and distal contacts. Preliminary results show that contact on the proximal link can be reliably detected, but further study is required. Additionally, we will examine the benefit from the use of two accelerometers, one mounted on the proximal link and one on the distal link. The addition of a second accelerometer will provide additional information about the system through additional measurements such as the phase difference between the two signals. This in turn could be used to further quantify measurements such as localizing the contact location.

Finally, we will examine alternative signal processing methods on the accelerometer data, considering amplitude-based metrics, as well as directly considering phase changes in the signal.

D. Conclusions

In this paper we present a novel approach to contact sensing that uses low cost integrated circuit components and the existing actuator and is capable of detecting contact at forces between 0.05 and 0.15 N on both faces of the digit. Unlike most other contact sensors, this approach does not involve instrumenting the surface of the digit with sensor arrays or construction of a specialized finger, making it easy to implement with existing finger designs. Although this work clearly demonstrates the validity of this approach to contact sensing, additional work is needed to further explore the sensor concept and optimize it for various applications such as contact detection for manipulation, workspace exploration, or safe operations in unstructured environments.

ACKNOWLEDGMENT

The authors would like to thank Lael Odhner and Rob Howe for their helpful discussions related to this work.

REFERENCES

[1] J. Tegin and J. Wikander, "Tactile sensing in intelligent robotic manipulation– - a review," *Industrial Robot: An International Journal,* vol. 32, pp. 64-70, 2005.

[2] G. Westling and R. Johansson, "Factors influencing the force control during precision grip," *Experimental Brain Research,* vol. 53, pp. 277-284, 1984.

[3] K. Motoo, F. Arai, and T. Fukuda, "Piezoelectric Vibration-Type Tactile Sensor Using Elasticity and Viscosity Change of Structure," *Sensors Journal, IEEE,* vol. 7, pp. 1044-1051, 2007.

[4] S. Omata and Y. Terunuma, "New tactile sensor like the human hand and its applications," *Sensors and Actuators A: Physical,* vol. 35, pp. 9-15, 1992.

[5] A. M. Dollar, L. P. Jentoft, J. H. Gao, and R. D. Howe, "Contact sensing and grasping performance of compliant hands," *Autonomous Robots,* vol. 28, pp. 65-75, 2010.

[6] P. Yong-Lae, K. Chau, R. J. Black, and M. R. Cutkosky, "Force Sensing Robot Fingers using Embedded Fiber Bragg Grating Sensors and Shape Deposition Manufacturing," in *Robotics and Automation, 2007 IEEE International Conference on*, 2007, pp. 1510-1516.

[7] H. Maekawa, K. Tanie, and K. Komoriya, "A finger-shaped tactile sensor using an optical waveguide," in *Systems, Man and Cybernetics, 1993. 'Systems Engineering in the Service of Humans', Conference Proceedings., International Conference on*, 1993, pp. 403-408 vol.5.

[8] A. M. Dollar and R. D. Howe, "A robust compliant grasper via shape deposition manufacturing," *Mechatronics, IEEE/ASME Transactions on,* vol. 11, pp. 154-161, 2006.

[9] H. Yousef, M. Boukallel, and K. Althoefer, "Tactile sensing for dexterous in-hand manipulation in robotics--A review," *Sensors and Actuators A: Physical,* 2011.

[10] C. Rudolf and W. Seemann, "Resonant Excitation of a Composite Beam using Piezoelectric MFC Actuators " presented at the Actuator 2008.